

Planning in Learned Latent Action Spaces for Generalizable Legged Locomotion

Tianyu Li
Facebook AI Research
USA
tianyul@fb.com

Roberto Calandra
Facebook AI Research
USA
rcalandra@fb.com

Deepak Pathak
CMU
USA
dpathak@cs.cmu.edu

Yuandong Tian
Facebook AI Research
USA
yuandong@fb.com

Franziska Meier
Facebook AI Research
USA
fmeier@fb.com

Akshara Rai
Facebook AI Research
USA
akshararai@fb.com

Abstract: Hierarchical learning has been successful at learning generalizable locomotion skills on walking robots in a sample-efficient manner. However, the low-dimensional “latent” action used to communicate between different layers of the hierarchy is typically user-designed. In this work, we present a fully-learned hierarchical framework, that is capable of jointly learning the low-level controller and the high-level action space. Next, we plan over latent actions in a model-predictive control fashion, using a learned high-level dynamics model. This framework is generalizable to multiple robots, and we present results on a Daisy hexapod simulation, A1 quadruped simulation, and Daisy robot hardware. We compare a range of learned hierarchical approaches, and show that our framework is more reliable, versatile and sample-efficient. In addition to learning approaches, we also compare to an inverse-kinematics (IK) based footstep planner, and show that our fully-learned framework is competitive in performance with IK under normal conditions, and outperforms it in adverse settings. Our hardware experiments show the Daisy hexapod achieving multiple locomotion tasks, such as goal reaching, trajectory and velocity tracking in an unstructured outdoor setting, with only 2000 hardware samples.

Keywords: Hierarchical learning, Legged locomotion, Latent actions, Model-predictive control

1 Introduction

Traditional control techniques used in legged locomotion, like inverse dynamics require assumptions about the dynamics of the system, such as no slipping, and can lead to poor performance when these assumptions are violated. In contrast, learning-based approaches do not make strict assumptions about dynamics, but are sample-inefficient to train. As a result, several works propose to leverage hierarchy as a structure to learn locomotion skills scalable to real robots [1, 2, 3]. However, typically in hierarchical control literature, the action space used by the high-level controller to interact with the low-level controller is user-defined [2, 3, 4]. Such a user-defined action space can potentially be too restrictive for some tasks. For example, Tsounis et al. [3] constrain the space to be a particular footstep pattern, while a different gait might move faster; Frans et al. [4], Li et al. [2] constrain the low-level to be a pre-defined set of primitives, constraining performance to the quality and number of primitives.

In this work, we introduce a generalizable, fully-learned, hierarchical control framework that eliminates the need for pre-defined action spaces for the high-level controller. We start by learning a low-level policy and latent action inputs that can reproduce a set of expert controllers in simulation, using supervised learning. This step transforms the initially discrete experts into a continuous space,



Figure 1: Our method is generalizable and can directly be used with waypoint navigation methods to reach a desired goal. Here, we present a snapshot showing our test platform ‘Daisy’ navigating a cluttered photo-realistic indoor simulation environment in iGibson [5] by following a collision-free path to goal. Our approach can follow the desired path, despite disturbances such as slipping and collisions with the environment.

allowing us to go beyond the initial finite number of primitives. For the high level controller, we propose a model-based planner, similar to Li et al. [2], and plan a sequence of continuous learned latent actions to achieve a desired goal. We learn a ‘coarse’ dynamics model of the center of mass of the robot over one cycle of the low-level policy given a latent action input, and use it for model-predictive control. This results in a reactive approach that continuously modulates the robot motion to achieve changing targets, responds to disturbances, and generalizes to multiple tasks.

We evaluate our approach on two legged locomotion robot simulations and one real robot. Our model-based planner, acting on a learned latent action space, outperforms prior hierarchical approaches in all evaluation tasks, while being more sample efficient. Furthermore, we compare our method with a traditional control technique based on inverse-kinematics (IK) with footstep planning, which is rarely addressed as a baseline method in hierarchical learning. Our approach performs comparably to IK in normal conditions, and outperforms it in adverse settings. Finally, we demonstrate that our approach can be used to solve complex locomotion tasks in a sample-efficient manner in the real world with a Daisy hexapod robot, with just 2000 hardware samples.

The main contributions of this work are: 1) Present a sample-efficient fully-learned hierarchical framework for locomotion and deploy it on a legged-robot. 2) A model-based planner over continuous latent actions. 3) An extensive comparison between different learned as well as traditional hierarchical control schemes. To the best of our knowledge, this is the first fully-learned model-based hierarchical framework demonstrated on a robot hardware, and multiple locomotion robot simulations. We believe the generalizability and sample-efficiency of our approach makes it highly suitable for solving long-term legged locomotion problems, such as indoor navigation (Figure 1).

2 Background and Related Work

Model predictive control We consider a Markov Decision Process with actions \mathbf{a} and states \mathbf{s} . Sampling an action \mathbf{a}_t at state \mathbf{s}_t , the agent measures a cost $c(\mathbf{s}_t, \mathbf{a}_t)$ and transitions to the next state $\mathbf{s}_{t+1} = f_{dyn}(\mathbf{s}_t, \mathbf{a}_t)$, starting from an initial state \mathbf{s}_0 . The objective of model-predictive control (MPC) is to minimize the long term cost of a trajectory $J = \sum_{t=0}^T \mathbb{E}_\tau [c(\mathbf{s}_t, \mathbf{a}_t)]$ with respect to the actions $\mathbf{a}_{0:T}$, given the dynamics $f_{dyn}(\mathbf{s}_t, \mathbf{a}_t)$. MPC plans a sequence of actions over a horizon H , starting from current state \mathbf{s}_{curr} as $\mathbf{a}_{0:H} = \arg \min_{\mathbf{a}_{0:H}} \sum_{h=0}^H c(\mathbf{s}_h, \mathbf{a}_h)$, given $\mathbf{s}_{h+1} = f_{dyn}(\mathbf{s}_h, \mathbf{a}_h)$ and $\mathbf{s}_0 = \mathbf{s}_{curr}$. The first action a_0 is applied, and the process repeats, starting with the new current state. MPC has been used in locomotion research, such as in Koenemann et al. [6], Mason et al. [7], Herdt et al. [8]. In this work, we learn the transition dynamics f_{dyn} from data, over a temporally-extended action sequence $\mathbf{a}_{1:N}$ of length N , i.e., $\mathbf{s}_{t+N} = f_{dyn}(\mathbf{s}_t, \mathbf{a}_{t:t+N})$. Similar dynamics models are used in Morimoto et al. [9] over Poincare sections of a bipedal gait.

Learning for locomotion Classical locomotion control techniques like [10] need knowledge of the dynamics of the robot, while machine learning approaches can learn locomotion without modelling dynamics [11]. Successful dynamics skills have been learned and applied on robots using domain randomization, and other sim2real approaches. Peng et al. [12], Tan et al. [13], Li et al. [14] learn a policy and a latent input iteratively in simulation, and optimize the latent input on hardware using Bayesian optimization. While these approaches can learn to walk, they do not generalize to multiple targets, such as reaching goals, and different velocities. In contrast, hierarchical decomposition

of control holds the promise of solving complex locomotion tasks in a generalizable manner. For instance, Kuindersma et al. [10], Kalakrishnan et al. [15], Feng et al. [16] decompose the problem of controlling a humanoid robot to center of mass planning, followed by model-based controllers. Frans et al. [4] demonstrate jointly learning the low-level and high-level policies in simulation, with a discrete set of low-level primitives. Yang et al. [17] learn low-dimensional pattern generator parameters and use them for high-level navigation. Tsounis et al. [3] use a learned high-level controller to decide a footstep location for a learned low-level policy. Hierarchical approaches have also been demonstrated on real robots, for example Li et al. [2] use a high-level controller to sequence a set of pre-learned primitives and Nachum et al. [1] use the high-level policy to define sub-goals for the low-level policy. However, these works assume a known high-level action space that communicates between the high-level and the low-level policies. This can be restrictive if the pre-defined action space is not complex enough to represent a task. In contrast, we present a framework that can learn a continuous space of low-level primitives along with a learned high-level input, and combine this with a model-based high-level planner to achieve multiple locomotion tasks.

Latent space learning for control There has been a lot of interest in the robotics community in learning latent representations of a task, and using them for control, such as Watter et al. [18], Banijamali et al. [19], Finn et al. [20] and Zhang et al. [21]. Latent state representations can compress high-dimensional state such as images into a low-dimensional state, hence are conducive for control. However, there are relatively fewer works that deal with latent actions, or latent inputs to a policy (without transition dynamics). Most closely related to our work is the work by Yu et al. [22], [23]. These works iteratively learn a policy and a latent input to the policy on a large range of environments in simulation, and fine-tune the latent input on hardware using Bayesian optimization. In contrast to these approaches, we jointly learn a latent input representation from a high-level policy to a low-level policy in a hierarchical setting. We use model-predictive control to plan over latent actions, allowing us to change the latent input to our low-level policy, on the fly. As a result, each hardware trajectory in our approach can have different latent inputs per step, as needed by the task, while the latent input is kept fixed in [22, 23] for each hardware rollout. This allows us to respond to online disturbances and reach arbitrary changing goals.

3 Hierarchical reinforcement learning for planning in locomotion

Our hierarchical learning framework, illustrated in Figure 2, consists of two steps: 1) Joint optimization of a low-level policy π_θ , and a latent action \mathbf{z} , using supervised learning. 2) Learning a dynamics model given the learned low-level policy $\pi_\theta(\cdot, \mathbf{z})$ over randomly sampled \mathbf{z} . 3) Model-based planning over \mathbf{z} using MPC. This method can generalize to multiple robots and locomotion tasks while remaining sample-efficient.

3.1 A hierarchical planning framework for locomotion

We divide the control of legged robots into a low-level policy and a high-level model-based planner. The low-level policy π_θ runs at a frequency of 100Hz and its behaviour is modulated by a latent input \mathbf{z} from the high-level planner, resulting in different behaviors on the robot. One popular example of this architecture is designing the low-level policy with inverse kinematics, and choosing high-level actions as footsteps. In contrast, we present a framework to learn the low-level policy, and latent input space without expert design. We also compare our method with the popular inverse kinematics setting in Section 4. The hyperparameters we use are listed in the appendix A.2.

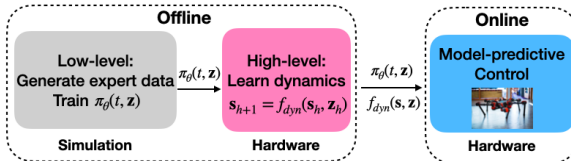


Figure 2: Flowchart explaining the learning pipeline of our proposed approach. (1) We learn a low-level policy $\pi_\theta(t, z)$ from expert controllers in simulation, where t characterizes the phase of movement, and z is the latent action. (2) We learn the high-level dynamics $s_{h+1} = f_{dyn}(s_h, z_h)$ that predicts the state changes after a latent action z_h is executed. (3) With π_θ and f_{dyn} , we run MPC on high-level for planning.

Low-level policy Our low-level policy is parametrized by a neural network that takes a phase variable $t \in (0, 1]$ as input, along with a latent action \mathbf{z} from the high-level planner. $\mathbf{q}_{des,t} =$

$\pi_\theta(t, \mathbf{z})$, $t = \frac{n}{N}$ where n is the current time step, which goes up to the primitive length N , at which point it is reset to 0 again. $\mathbf{q}_{des,t}$ are the desired joint-angles sent to the robot. The phase t is linearly increased through a pre-determined primitive length N , and ensures a cyclic nature of the low-level policy. For a fixed \mathbf{z} , the policy generates the same joint angle pattern every N time steps in a periodic manner.

High-level planner We use a model-based high-level planner that plans a latent action sequence $\mathbf{z}_{1:H}$ for our planning horizon H using MPC. The dynamics used in this planning are learned over a primitive cycle of length N , rather than the instantaneous dynamics, i.e. $s_{t+N} = f_{dyn}(s_t, \mathbf{z}_t)$ is the next state after executing the low-level policy for N time steps, starting from s_t , with latent action \mathbf{z}_t . This leads to a ‘coarse’ dynamics model learned over extended low-level action sequences, rather than per time step transitions. Starting from the current center of mass (CoM) position and orientation $s_{curr} = (\mathbf{x}_{com}, \theta_{com})$, our high level planner does a search over the possible sequences of actions to find the optimal sequence for our horizon of H : $\mathbf{z}_{1:H} = \arg \min_{\mathbf{z}_{1:H}} \sum_{h=1}^H c_{hl}(s_h, \mathbf{z}_h)$ such that $s_{h+1} = f_{dyn}(s_h, \mathbf{z}_h)$ and $s_0 = s_{curr}$. c_{hl} is the high-level cost function; h is a robot step, consisting of N time steps. The first action \mathbf{z}_1 is applied on the robot, and the optimization is repeated, starting from the new state. We optimize the MPC cost by randomly sampling 2000 actions, over a horizon of $H = 1$ and pick the best action. The cost is designed by the user depending on the task at hand, described in Section 4.1.

3.2 Jointly learning low-level policy and latent actions

We propose a joint learning framework for learning a low-level policy and latent actions, starting with G expert controllers. We use supervised learning to jointly optimize a low-level policy π_θ and a latent action \mathbf{z} input into π_θ that leads to a desired expert behavior π^{exp} . Specifically, we optimize θ and one latent action per expert \mathbf{z}_g , such that $\pi_\theta(\cdot, \mathbf{z}_g)$ matches the corresponding expert: $\pi_\theta(t, \mathbf{z}_g) = \pi_g^{exp}(t)$ for $g = 1 \dots G$. This ensures that, if trained properly, π_θ is capable of generating G experts, with different inputs \mathbf{z}_g per expert. This can be seen as a bottle-neck formulation where we want to jointly learn a representation of θ and \mathbf{z} such that a large range of gaits can be produced by the policy π_θ for different inputs \mathbf{z} . The loss for each gait g becomes $\mathcal{L}_g = \|\pi_\theta(t, \mathbf{z}_g) - \pi_g^{exp}(t)\|^2$. θ and $\mathbf{z}_{1:G}$ can now be optimized together to reduce the total loss $\mathcal{L} = \sum_{g=1}^G \|\pi_\theta(t, \mathbf{z}_g) - \pi_g^{exp}(t)\|^2$

$$\theta, \mathbf{z}_{1:G} = \arg \min_{\theta, \mathbf{z}_{1:G}} \sum_{g=1}^G \|\pi_\theta(t, \mathbf{z}_g) - \pi_g^{exp}(t)\|^2.$$

The partial derivatives of the total loss \mathcal{L} with respect to latent variable \mathbf{z}_g and the policy weights θ are:

$$\frac{\partial \mathcal{L}}{\partial \mathbf{z}_g} = \frac{\partial}{\partial \mathbf{z}_g} \|\pi_\theta(t, \mathbf{z}_g) - \pi_g^{exp}(t)\|^2, \quad \frac{\partial \mathcal{L}}{\partial \theta} = \frac{\partial}{\partial \theta} \sum_{g=1}^G \|\pi_\theta(t, \mathbf{z}_g) - \pi_g^{exp}(t)\|^2. \quad (1)$$

This naturally leads to a formulation where the update to each latent input \mathbf{z}_g is only affected by the supervised learning loss of the expert policy g that it is trying to mimic. On the other hand, updates to low-level policy parameters θ are optimized by reducing the loss over all G experts. This is in contrast to other approaches in literature such as [22, 12] that iteratively optimize the latent action and policy for different settings, and can lead to unstable training. Moreover, unlike [12] we learn a unified low-level policy across all experts, and not separate policies for different experts. Once π_θ is learned, we are no longer limited to the G experts that were used during training. By sampling in the space of latent actions \mathbf{z} , we can generate new controllers that interpolate, and extrapolate from the training experts. As illustrated in Figure 3, different \mathbf{z} lead to different CoM trajectories. Close-by samples in the latent action space leads to continuously varying behaviors in the CoM space, showing that our learned latent space is structured and stable.

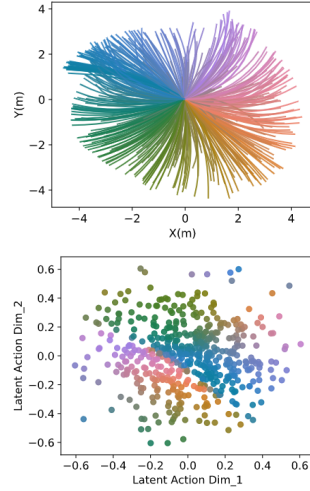


Figure 3: CoM Trajectory in XY plane caused by randomly sampling in a 2-dimensional latent space. Close-by samples in the latent space lead to continuously varying CoM motion.

3.3 Learning center of mass dynamics

Once the policy π_θ and latent space \mathbf{z} is learned, we can plan over \mathbf{z} to accomplish a variety of locomotion tasks, like reaching goals and trajectory tracking. To do this, we learn a temporally-extended dynamics model of the center of mass (CoM), learned by sampling a series of random latent actions \mathbf{z} and measuring the resultant CoM state after one cycle of the low-level policy $\pi_\theta(\cdot, \mathbf{z})$. In a similar spirit, previous works like Kuindersma et al. [10], Feng et al. [16] have used approximate CoM dynamics models such as a linear inverted pendulum (LIPM). Since LIPM is not the true dynamics of the robot, the desired CoM trajectory from LIPM might not be feasible on the robot. For example, the maximum leg length and CoM velocity of LIPM is artificially constrained to account for robot dynamics. However, we do not need to manually define these constraints in our setup, as the learned dynamics already include them. For example, the dynamics learn that certain latent actions result in slipping on the robot, and hence lead to slower CoM movement.

Formally, we represent current state of the CoM by $s_{curr} = (x_{curr}, y_{curr}, \gamma_{curr}, \dot{x}_{curr}, \dot{y}_{curr})$, where (x_{curr}, y_{curr}) is the current horizontal position, $(\dot{x}_{curr}, \dot{y}_{curr})$ is the current horizontal velocity and γ_{curr} is the current yaw. The learned dynamics represent a transition from the current state to the next state $s_{next} = (x_{next}, y_{next}, \gamma_{next}, \dot{x}_{next}, \dot{y}_{next})$, using the low-level controller π_θ with latent action \mathbf{z} . To simplify the learning, we learn a delta dynamics model.

$$\Delta x, \Delta y, \Delta \gamma, \dot{x}_{next}, \dot{y}_{next} = f_{dyn}(\dot{x}_{curr}, \dot{y}_{curr}, z) \quad (2)$$

$$\text{where } \Delta x = x_{next} - x_{curr}, \quad \Delta y = y_{next} - y_{curr}, \quad \Delta \gamma = \gamma_{next} - \gamma_{curr}. \quad (3)$$

In our experiments, we do not explicitly model the CoM dynamics in the vertical plane, or the roll and pitch of the robot, to improve sample-efficiency of dynamics learning. Implicitly, controllers with lower CoM height, or high roll and pitch lead to slower gaits. Explicitly modelling height, roll and pitch could lead to better control of height and orientation, and can be studied in the future.

4 Experiments

We evaluate our proposed framework on two robot simulations and one real robot. We provide extensive comparison to prior learning-based methods, as well as, an expert-designed control approach. Results demonstrate that our approach outperforms other approaches from literature, is not limited to a specific robot and can solve multiple real-world locomotion tasks.

4.1 Experimental Setup

We use Pybullet [24] as our physics simulator, and build models for two robots: Daisy hexapod robot from Hebi robotics [25] and A1 quadruped from Unitree Robotics [26], shown in Figure 4a and 4b respectively. Daisy is a 6-legged robot, with 3 motors in each leg, leading

to a total of 18 actuators. A1 is a 4-legged robot, with 3 motors in each leg, leading to a total of 12 actuators. On hardware, we use the Daisy robot with a Realsense tracking camera [27] to measure the position, orientation and velocity of the robot in an unstructured outdoor space. To evaluate our method, we create a series of tasks that are relevant to solving real-world locomotion problems.

Velocity tracking: This metric measures the robot’s ability to track a desired CoM velocity \mathbf{v}_{tgt} and orientation γ_{tgt} , leading to cost $c_1 = w_1 \|\mathbf{v}_{tgt} - \mathbf{v}_{curr}\| + w_2 \|\gamma_{tgt} - \gamma_{curr}\|$, where $[w_1, w_2] = [2, 1]$. The target velocity is varied throughout the experiment and the robot has to adapt its control to minimize the velocity error. Our target velocities are $[0.0, 0.2]$ m/s, $[0.2, 0.0]$ m/s, $[0.0, -0.2]$ m/s, $[-0.2, 0.0]$ m/s where each variable indicates desired velocity in x and y directions respectively.

Goal reaching: Quite a few real-world locomotion tasks involve reaching a goal in space, either as a long-distance goal, or an intermediate waypoint. We study the efficacy of control approaches to reach a range of targets in CoM location $s_{tgt} = (x_{tgt}, y_{tgt})$ and orientation γ_{tgt} using cost $c_2 =$

Algorithm 1: Learning latent actions with model-based planning

Given G expert policies $\pi_{1:G}^{exp}$, high-level cost c_{hl} , horizon H

Randomly initialize G latent actions $\mathbf{z}_{1:G}$, π_θ

for each gradient step do

 Update $\mathbf{z}_g, \pi_\theta = \arg \min_{z_g, \pi_\theta} \mathcal{L}(z_g, \theta)$,

$\mathcal{L} = \sum_{g=1}^G \|\pi_\theta(t, \mathbf{z}_g) - \pi_g^{exp}(t)\|$

for each dynamics learning step do

$\mathbf{z} \sim N(\mu, \sigma)$

while $t \leq N$ **do**

$\mathbf{q}_{des}(t) = \pi_\theta(t, \mathbf{z})$

$D \leftarrow D \cup \{(s_0, \mathbf{z}, \mathbf{s}_N)\}$

 Update dynamics model $\mathbf{s}_N = f_\alpha(s_0, \mathbf{z})$

$\mathbf{s}_0 \leftarrow \mathbf{s}_N$

for each planning step do

$\mathbf{z}_{1:H} = \arg \min c_{hl}(s_0, \mathbf{z}_{1:H})$

 Apply latent action \mathbf{z}_1 , measure \mathbf{s}_N

$\mathbf{s}_0 \leftarrow \mathbf{s}_N$

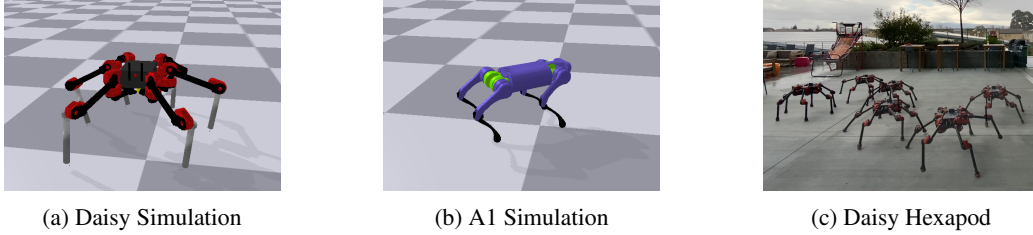


Figure 4: Our experimental platforms: Daisy in Pybullet, A1 in Pybullet, and a real-world Daisy.

$w_1 \|s_{tgt} - s_{curr}\| + w_2 \|\gamma_{tgt} - \gamma_{curr}\|$, where $[w_1, w_2] = [2, 1]$. The desired goals are eight points uniformly distributed on a circle of radius 2m, with target orientation always point towards y axis.

Trajectory tracking: For navigating cluttered spaces with obstacles, or controlled environments, like a road, it is important to closely follow a CoM trajectory designed by a planner. We track an S-shaped desired trajectory consisting of target positions $s_{tgt,t}$ and orientations $\gamma_{tgt,t}$ that change with time t , leading to cost $c_3 = w_1 \|s_{tgt,t} - s_{curr}\| + w_2 \|\gamma_{tgt,t} - \gamma_{curr}\|$, where $[w_1, w_2] = [2, 1]$.

4.2 Comparison experiments with hierarchical learning approaches in simulation

Several works have proposed hierarchical learning for locomotion, with a few demonstrations on hardware [1, 2]. To compare our approach against these prior approaches, we create an ablation experiment in simulation. We characterize all hierarchical approaches by the choice of their low-level and high-level policies, and sweep through the different choices made in literature. Finally we test all the approaches on two robot simulations and the tasks described in Section 4.1. Note that all model-free approaches had to be re-trained for new tasks, and hence, *effectively take 3 times as much data* as our approach. The approaches compared are shown in Figure 5 and can be broadly categorized into the following groups:

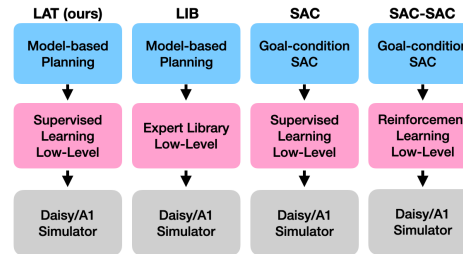


Figure 5: Flowchart of the different approaches from literature that we compare against.

A library of experts as a low-level policy (LIB): A popular choice in literature, such as in Li et al. [2], Nachum et al. [28], is to use a library of low-level experts, and learn a high-level policy that chooses between the experts. We consider the same library of experts that was used for supervised training of our low-level policy, and learn a model-based high-level policy, as in Li et al. [2].

Model-free high-level policy (SAC) with our low-level policy: An alternative to model-based policy is to learn a model-free high-level policy, as in Nachum et al. [1], [28]. As our test tasks involve generalization to multiple goals, we use goal-conditioned SAC to learn this high-level policy, assuming the same pre-learned low-level policy as our approach. This setting is also similar to [12] and [22], though these approaches cannot directly generalize to multiple targets.

Model-free learned low-level and high-level policy (SAC-SAC): Nachum et al. [1] use model-free RL for training a low-level policy designed to reach sub-goals, and train a model-free high-level policy to define sub-goals for the pre-trained low-level policy. We use goal-conditioned SAC to learn both levels of this hierarchy, first training the low-level, then training the high-level, keeping the low-level fixed.

The summary of our comparison experiments is shown in Figure 6c. All model-free approaches are trained on half of the test targets, and tested on all targets. For example, for goal reaching, high-level goal-conditioned SAC is trained on 4 goals, and tested on all 8. Moreover, each model-free approach is re-trained for new tasks, hence, effectively takes 3 times as much data as our approach for achieving these tasks. Our experiments show that both SAC and SAC-SAC baselines described above fail to generalize to new goal and trajectories, and perform worse than our approach on goal reaching and trajectory tracking tasks. On the other hand LIB uses a model-based high-level controller, like our approach, and generalizes well to these scenarios. For velocity tracking, however, the low-level primitives in LIB do not include experts that can reach the target velocity, and hence perform worse

than our approach. This highlights that our approach combines the robustness of model-based controllers with generalizable continuous low-level primitives, and can successfully solve a large range of tasks without any additional data.

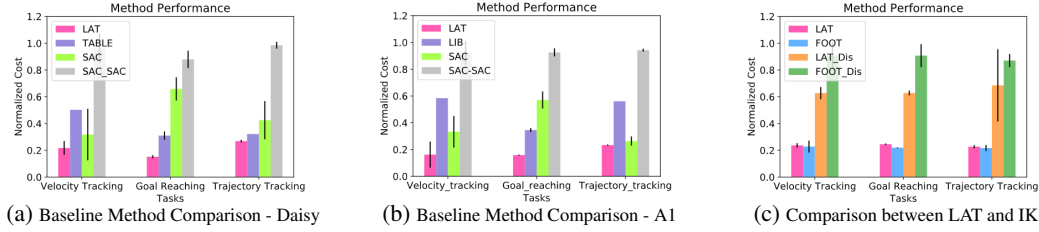


Figure 6: A comparison of the approaches mentioned in Figure 5 on different experimental settings and two robot simulators. Our framework with a model-based high-level planner and supervised learning for low-level policy outperforms other method in all test tasks. The hyperparameters used are listed in A.2.

4.3 Comparisons with a structured controller in simulation

Next, we present a comparison between our fully-learned hierarchical scheme, and a structured hierarchical control scheme, consisting of planning footsteps, and achieving them with inverse kinematics (IK). Similar control schemes have been shown to be successful at achieving a large range of locomotion tasks, as in [10]. Using footsteps instead of a learned latent action is an easy change for our setup, where the low-level policy π_θ is replaced by IK, and the high-level action \mathbf{z} is replaced by footsteps. A high-level planner uses a learned CoM transition dynamics model, similar to Section 3.1, with desired footsteps as the ‘latent’ action.

Inverse kinematics (IK) is effective when the kinematics of the robot are known, but it might suffer when kinematic assumptions are violated. In such scenarios, learned models and policies might be advantageous. With this in mind, we run comparison experiments with IK in the normal setting, as well as, an adverse setting where two back robot legs are disabled by fixing their joint angles in simulation. The results are summarized in Figure 6b for Daisy simulation, and show that our fully-learned approach is close to IK in the normal setting. However, when the two hind legs are disabled, IK’s performance deteriorates significantly, while our learned latent space compensates for this adverse setting, and outperforms IK.

4.4 Hardware experiments on Daisy Hexapod

Next, we describe the performance of our proposed approach on the Daisy robot hardware. Transfer to hardware is straight-forward for our approach, once the latent action space and low-level policy have been learned in simulation. We keep the low-level policy and latent action space from simulation fixed on hardware, and learn the CoM dynamics by randomly sampling latent actions. Once the dynamics model is learned, it is kept fixed, as we conduct hardware experiments, which span multiple days. Since our hardware experiments are conducted outdoors, in an uncontrolled environment, they naturally include noise due to tracking errors by the Realsense camera, slipping on gravel, joint tracking and ground height disturbances. We use 2000 hardware samples for fitting the dynamics model, and 20 simulation expert controllers for learning the low-level policy. The performance of our approach on hardware is shown in Figure 7. For goal reaching, our approach could reach all goals in 16.0 ± 1.4 steps, averaged over 4 goals and 3 trials. The velocity tracking error on hardware was 0.56 ± 0.015 and trajectory tracking error was 0.57 ± 0.05 .

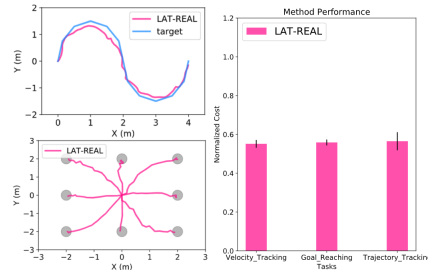


Figure 7: Performance on real world Daisy Hexapod. Here we show the goal reaching task (left-top), and trajectory tracking (left-bottom). (Right) Costs for each task over 3 hardware runs.

While our approach was able to track the desired trajectory, and reach desired goals, its overall performance deteriorated on hardware. This was due to a few reasons: the number of samples used for learning dynamics on hardware were 1/5 of the samples used in simulation, leading to a bad dynamics model, and hence worse planning. Moreover, learning the dynamics on hardware was much

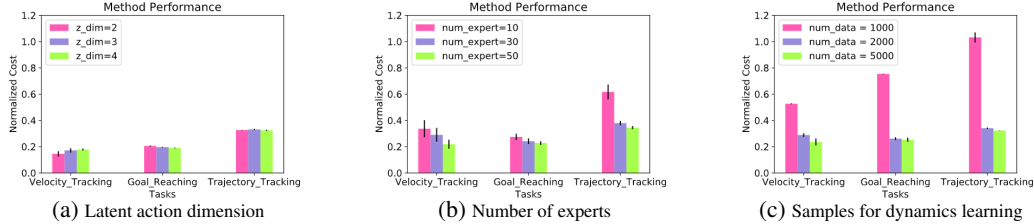


Figure 8: Result of ablation study on sensitivity of different hyperparameters. Our approach is not sensitive to hyperparameters once a reasonably good dynamics model and low-level policy has been learned.

harder due to noise from poor joint tracking, slipping and sensory noise in CoM estimation. Both of these issues can be alleviated by using more hardware samples for learning the CoM dynamics model, or starting from a simulation dynamics model and fine-tuning. Additionally, we observed that the robot was unable to achieve some high velocity targets, as the low-level controllers that could achieve high velocities in simulation did not transfer to hardware. This was because simulation does not sufficiently capture the motor bandwidth of the robot, but the gap can potentially be reduced by using experts learned using domain-randomization. Despite these sim-to-real challenges, our method was able to achieve all target goals, and follow the desired trajectory.

4.5 Ablation study on hyperparameters

Lastly, we conduct an ablation experiment where we change the dimension of our latent space, number of expert controllers and number of samples used in training the dynamics model in Daisy simulation. We vary the latent action dimensions to be 2, 3, 4, while keeping all other hyperparameters fixed, and find that there is no significant effect on the performance. Next, we use different numbers of expert controllers – 10, 30, 50 experts – for training the low level policy. As the number of experts increases the performance on each tasks improves, though the difference from 30 to 50 is minor. Lastly, we vary the number of samples used for learning the dynamics high-level model, using 1000, 2000 and 5000 datapoints. We observe that there is a significant improvement in performance when the dynamics is learned from 2000 data points versus 1000, showing that a better dynamics models leads to better generalization. However, there is no significant difference in performance between 2000 and 5000 data points, signifying that our approach is not sensitive to accurate dynamics model, and can perform well with a small number of samples. The result are summarized in Figure 8, and each test setting is averaged over 10 independent trials.

5 Discussion

Diversity of expert gaits for low-level training: For our hardware experiments, we used 20 experts from simulation to learn the low-level policy. The richness of the expert library directly affects the performance of the low-level controller, and since some of the low-level controllers did not transfer to hardware, the performance of our approach suffered. One of the challenges of our approach is to build a sufficiently diverse low-level policy, that can transfer to hardware and perform well. A combination of curiosity-driven policy learning, and dynamics randomization [13] might be helpful.

Learning high-level dynamics models on hardware: Since our high-level dynamics models did not include the full state of the robot, they could not account for the differences caused by different initial conditions at the start of the step. For example, when the robot had poor joint angle tracking, the CoM height reduced on each step, causing slower movement. Incorporating the full joint state would eliminate this issue, but also make the dynamics learning much more sample-inefficient. On uneven ground, information about terrain also becomes important in learning the high-level dynamics. This motivates learning a dynamics model that can incorporate high-dimensional state information into a low-dimensional latent state space, followed by learning in this reduced space.

6 Conclusions

In this paper, we present a hierarchical control framework for planning a sequence of learned latent actions from a high-level controller to a low-level policy. This framework allows us to accomplish several real-world locomotion tasks, such as goal-reaching, trajectory and velocity tracking

with only 2000 samples on hardware. We present comparisons of our approach to other hierarchical control approaches from literature – including both learned and expert-designed traditional approaches, on two robot simulations. Our approach outperforms prior learning-based approaches on all tasks and performs similar to the expert-designed approach in normal settings while outperforming it when two hind legs are disabled in simulation. This work demonstrates the efficacy of a fully-learned hierarchical framework at achieving various locomotion tasks, and solving real-world problems like navigation. It removes the need for user-designed pattern generators, or hierarchical decomposition, and opens up avenues for further research such as discovering new gaits, enabling sim-to-real transfer without performance loss, and navigating unknown terrains autonomously.

References

- [1] O. Nachum, M. Ahn, H. Ponte, S. Gu, and V. Kumar. Multi-agent manipulation via locomotion using hierarchical sim2real. *arXiv preprint arXiv:1908.05224*, 2019. URL <https://arxiv.org/abs/1908.05224>.
- [2] T. Li, N. Lambert, R. Calandra, F. Meier, and A. Rai. Learning generalizable locomotion skills with hierarchical reinforcement learning. *arXiv preprint arXiv:1909.12324*, 2019. URL <https://arxiv.org/abs/1909.12324>.
- [3] V. Tsounis, M. Alge, J. Lee, F. Farshidian, and M. Hutter. Deepgait: Planning and control of quadrupedal gaits using deep reinforcement learning. *arXiv preprint arXiv:1909.08399*, 2019. URL <https://arxiv.org/abs/1909.08399>.
- [4] K. Frans, J. Ho, X. Chen, P. Abbeel, and J. Schulman. Meta learning shared hierarchies. *arXiv preprint arXiv:1710.09767*, 2017. URL <https://arxiv.org/abs/1903.01390>.
- [5] F. Xia, W. B. Shen, C. Li, P. Kasimbeg, M. E. Tchapmi, A. Toshev, R. Martín-Martín, and S. Savarese. Interactive gibbon benchmark: A benchmark for interactive navigation in cluttered environments. *IEEE Robotics and Automation Letters*, 5(2):713–720, 2020.
- [6] J. Koenemann, A. Del Prete, Y. Tassa, E. Todorov, O. Stasse, M. Bennewitz, and N. Mansard. Whole-body model-predictive control applied to the hrp-2 humanoid. In *2015 IEEE/RSJ International Conference on Intelligent Robots and Systems (IROS)*, pages 3346–3351. IEEE, 2015. URL <https://ieeexplore.ieee.org/document/7353843>.
- [7] S. Mason, N. Rotella, S. Schaal, and L. Righetti. An mpc walking framework with external contact forces. In *2018 IEEE International Conference on Robotics and Automation (ICRA)*, pages 1785–1790. IEEE, 2018. URL <https://arxiv.org/abs/1712.09308>.
- [8] A. Herdt, H. Diedam, P.-B. Wieber, D. Dimitrov, K. Mombaur, and M. Diehl. Online walking motion generation with automatic footstep placement. *Advanced Robotics*, 24(5-6):719–737, 2010. URL <https://hal.inria.fr/inria-00391408v1/document>.
- [9] J. Morimoto, J. Nakanishi, G. Endo, G. Cheng, C. G. Atkeson, and G. Zeglin. Poincare-map-based reinforcement learning for biped walking. In *2005 IEEE International Conference on Robotics and Automation*, pages 2381–2386. IEEE, 2005. URL <https://ieeexplore.ieee.org/document/1570469>.
- [10] S. Kuindersma, R. Deits, M. Fallon, A. Valenzuela, H. Dai, F. Permenter, T. Koolen, P. Marion, and R. Tedrake. Optimization-based locomotion planning, estimation, and control design for the atlas humanoid robot. *Autonomous robots*, 40(3):429–455, 2016. URL <https://link.springer.com/article/10.1007/s10514-015-9479-3>.
- [11] T. Haarnoja, S. Ha, A. Zhou, J. Tan, G. Tucker, and S. Levine. Learning to walk via deep reinforcement learning. *arXiv preprint arXiv:1812.11103*, 2018. URL <https://arxiv.org/pdf/1812.11103.pdf>.
- [12] X. Peng, E. Coumans, T. Zhang, T.-W. E. Lee, J. Tan, and S. Levine. Learning agile robotic locomotion skills by imitating animals. 07 2020. doi:10.15607/RSS.2020.XVI.064.

- [13] J. Tan, T. Zhang, E. Coumans, A. Iscen, Y. Bai, D. Hafner, S. Bohez, and V. Vanhoucke. Sim-to-real: Learning agile locomotion for quadruped robots. *arXiv preprint arXiv:1804.10332*, 2018. URL <https://arxiv.org/pdf/1804.10332.pdf>.
- [14] T. Li, H. Geyer, C. G. Atkeson, and A. Rai. Using deep reinforcement learning to learn high-level policies on the atrias biped. In *2019 International Conference on Robotics and Automation (ICRA)*, pages 263–269. IEEE, 2019.
- [15] M. Kalakrishnan, J. Buchli, P. Pastor, M. Mistry, and S. Schaal. Learning, planning, and control for quadruped locomotion over challenging terrain. *The International Journal of Robotics Research*, 30(2):236–258, 2011. URL <https://journals.sagepub.com/doi/abs/10.1177/0278364910388677>.
- [16] S. Feng, E. Whitman, X. Xinjilefu, and C. G. Atkeson. Optimization-based full body control for the darpa robotics challenge. *Journal of Field Robotics*, 32(2):293–312, 2015. URL <https://onlinelibrary.wiley.com/doi/abs/10.1002/rob.21559>.
- [17] B. Yang, G. Wang, R. Calandra, D. Contreras, S. Levine, and K. Pister. Learning flexible and reusable locomotion primitives for a microrobot. *IEEE Robotics and Automation Letters*, 3(3):1904–1911, 2018. URL <https://arxiv.org/abs/1803.00196>.
- [18] M. Watter, J. Springenberg, J. Boedecker, and M. Riedmiller. Embed to control: A locally linear latent dynamics model for control from raw images. In *Neural Information Processing Systems*, pages 2746–2754, 2015. URL <https://arxiv.org/abs/1506.07365>.
- [19] E. Banijamali, R. Shu, M. Ghavamzadeh, H. Bui, and A. Ghodsi. Robust locally-linear controllable embedding. *arXiv preprint arXiv:1710.05373*, 2017. URL <https://arxiv.org/abs/1710.05373>.
- [20] C. Finn, X. Y. Tan, Y. Duan, T. Darrell, S. Levine, and P. Abbeel. Deep spatial autoencoders for visuomotor learning. In *2016 IEEE International Conference on Robotics and Automation (ICRA)*, pages 512–519. IEEE, 2016.
- [21] M. Zhang, S. Vikram, L. Smith, P. Abbeel, M. J. Johnson, and S. Levine. Solar: deep structured representations for model-based reinforcement learning. *arXiv preprint arXiv:1808.09105*, 2018. URL <http://proceedings.mlr.press/v97/zhang19m/zhang19m.pdf>.
- [22] W. Yu, J. Tan, Y. Bai, E. Coumans, and S. Ha. Learning fast adaptation with meta strategy optimization. *arXiv preprint arXiv:1909.12995*, 2019. URL <https://arxiv.org/abs/1909.12995>.
- [23] W. Yu, V. C. Kumar, G. Turk, and C. K. Liu. Sim-to-real transfer for biped locomotion. *arXiv preprint arXiv:1903.01390*, 2019. URL <https://arxiv.org/abs/1903.01390>.
- [24] E. Coumans and Y. Bai. Pybullet, a python module for physics simulation for games, robotics and machine learning. <http://pybullet.org>, 2016–2019. URL <https://mitpress.mit.edu/books/legged-robots-balance>.
- [25] Hebi robotics. <https://www.hebirobotics.com/robotic-kits>.
- [26] Unitree robotics. <http://www.unitree.cc/>.
- [27] Realsense tracking camera. <https://www.intelrealsense.com/tracking-camera-t265/>.
- [28] O. Nachum, S. S. Gu, H. Lee, and S. Levine. Data-efficient hierarchical reinforcement learning. In *Advances in Neural Information Processing Systems*, pages 3303–3313, 2018.

A Appendix

A.1 Footstep Planning Control

We provide some details on the footstep planner used as a baseline in our work. To calculate the desired footstep, we take the desired center of mass displacement (CoM) and orientation $(\Delta x_{com}, \Delta y_{com}, \Delta \gamma_{com})$, current location of the foot in CoM frame $(x_{f,curr}, y_{f,curr}, \gamma_{f,curr})$ and convert it to a desired footstep for each foot, assuming a tripod gait.

$$\begin{aligned}\Delta x_f &= \Delta x_{com} + r \cdot [\cos(\gamma_{f,curr} + \Delta \gamma_{com}) - \cos(\gamma_{f,curr})] \\ \Delta y_f &= \Delta y_{com} + r \cdot (\sin(\gamma_{f,curr} + \Delta \gamma_{com}) - \sin(\gamma_{f,curr})) \\ r &= \sqrt{x_{f,curr}^2 + y_{f,curr}^2} \\ x_{f,des} &= x_{f,curr} + \Delta x_f, \quad y_{f,des} = y_{f,curr} + \Delta y_f\end{aligned}$$

The desired footstep locations are passed through a footstep trajectory generator (linear trajectory in horizontal plane, sinusoidal in vertical plane), and followed using inverse kinematics. This results in a desired footstep location that directly takes into account the desired orientation and displacement of the CoM. In our experiments, we find that such a representation of footstep planning can lead to a very fine control of CoM orientation and stable movement.

A.2 Training Hyperparameters

Here we list the hyperparameters we use for baseline method comparison.

	LAT	LIB	SAC	SAC-SAC
High Level NN size	512*2		512*2	512*2
Low Level NN size	512*2		512*2	512*2
Number of samples	10000	500	10000*3	10000*3
Batch size	512		512	512
Optimizer	Adam		Adam	Adam
Learning rate	1e-3		1e-3	1e-3